Influences of annealing on structural and compositional properties of Al_2O_3 thin films grown on 4H–SiC by atomic layer deposition*

Li-Xin Tian(田丽欣), Feng Zhang(张峰)†, Zhan-Wei Shen(申占伟), Guo-Guo Yan(闫果果), Xing-Fang Liu(刘兴昉), Wan-Shun Zhao(赵万顺), Lei Wang(王雷), Guo-Sheng Sun(孙国胜), and Yi-Ping Zeng(曾一平)

Key Laboratory of Semiconductor Material Sciences, Beijing Key Laboratory of Low Dimensional Semiconductor Materials and Devices, Institute of Semiconductors, Chinese Academy of Sciences, Beijing 100083, *China*

(Received 25 March 2016; revised manuscript received 8 August 2016; published online 25 October 2016)

Annealing effects on structural and compositional performances of Al_2O_3 thin films on 4H–SiC substrates are studied comprehensively. The Al_2O_3 films are grown by atomic layer deposition through using trimethylaluminum and H_2O as precursors at 300 °C, and annealed at various temperatures in ambient N_2 for 1 min. The Al_2O_3 film transits from amorphous phase to crystalline phase as annealing temperature increases from 750 °C to 768 °C. The refractive index increases with annealing temperature rising, which indicates that densification occurs during annealing. The densification and grain formation of the film upon annealing are due to crystallization which is relative with second-nearest-neighbor coordination variation according to the x-ray photoelectron spectroscopy (XPS). Although the binding energies of Al 2p and O 1s increase together during crystallization, separations between Al 2p and O 1s are identical between as-deposited and annealed sample, which suggests that the nearest-neighbour coordination is similar.

Keywords: atomic layer deposition, annealing, transition, 4H–SiC

PACS: 81.40.Ef, 68.55.–a **DOI:** 10.1088/1674-1056/25/12/128104

1. Introduction

Silicon carbide (SiC) is a promising candidate for high-temperature, high-voltage and high-power devices due to its wide band gap, high critical electric field, thermal and chemical stability.[1] Recently, Al_2O_3 acting as gate dielectric on a 4H–SiC metal–oxide–semiconductor (MOS) device was studied and reported by several groups.[2–4] Compared with widely used SiO_2 and Si_3N_4 on 4H–SiC, the Al_2O_3 in MOS device has advantages of large relative dielectric constant (~ 9), low interface-state density, and high mobility.[5–7]

Atomic layer deposition (ALD) is an attractive tool to deposit dielectric thin films on various substrates.[8] The self-terminating growth is an outstanding feature of ALD, because of which such films obtained by ALD are uniform in thickness and conformal even in high aspect ratio structures. Moreover, thickness of film is strictly controlled by the number of reaction cycles. In recent years, the ALD process has contributed to the development of microelectronic devices largely.[9] Several studies of Al_2O_3 deposited on SiC have reported the presence of defect states like Al–Al and –OH bonds in the Al_2O_3 films grown by ALD.[4,10,11] Avice *et al.*[2] and Tanner *et al.*[12] both focused on the interface between Al_2O_3 and SiC, but obtained distinct results. Avice *et al.* demonstrated that a transition layer appears between Al_2O_3 and SiC after being annealed as indicated by the results from TEM and x-ray photoelectron spectroscopy (XPS). However, the results of TEM in Ref. [12] indicated an abrupt interface between Al_2O_3 and 4H–SiC. In our paper, we study the interface between Al_2O_3 and SiC mainly by XPS analysis.

Rapid thermal annealing (RTA) is a desktop rapid thermal processor by using high-intensity, visible radiation to heat a single wafer for a short time at precisely controlled temperatures. One of the characteristics of RTP is to precisely adjust the time–temperature profile according to the required suitable specific process. Precise temperature position helps us realize annealing at a series of temperatures with small intervals and thus ensuring the reliability of the crystallization determination.

Although the deposition of Al_2O_3 on SiC by using the ALD has been investigated and examined as mentioned above, rapid thermal annealing (RTA) effects on structural (from amorphous to crystalline) and compositional transitions of ALD Al_2O_3 as annealing temperature rises have not been studied comprehensively.

In this paper, Al_2O_3 dielectric films are deposited on SiC epitaxial wafers by ALD to investigate the structural and compositional transitions of Al_2O_3 films at different annealing temperatures. The physical and chemical mechanisms of the transitions are examined, which can be a significant reference for Al_2O_3 dielectric films to be applied in power and microelectronic fields.

*Project supported by the National Basic Research Program of China (Grant No. 2015CB759600), the National Natural Science Foundation of China (Grant Nos. 61474113, 61574140, and 61274007), and the Beijing Nova Program, China (Grant No. xx2016071), and the CAEP Microsystem and THz Science and Technology Foundation (Grant No. CAEPMT201502).

†Corresponding author. E-mail: fzhang@semi.ac.cn

© 2016 Chinese Physical Society and IOP Publishing Ltd

2. Experiment

Al_2O_3 dielectric was grown by ALD on Si face, n-type 4H–SiC wafer with a 10-μm thick epilayer (doping level of 2×10^{15} cm^{-3}) on a highly doped substrate oriented 4° off the (0001) direction. Prior to growth, the epitaxial wafer was cleaned by Radio Corporation of America (RCA) process. Dilute hydrofluoric acid (1:20 HF:DI) was also used to remove native oxide on 4H–SiC surface. Then Al_2O_3 gate dielectric was deposited on 4H–SiC epitaxial wafer by a home-made ALD at 300 °C by using trimethylaluminum (TMA) and H_2O as precursors as well as N_2 as carrier gas. H_2O and TMA were pulsed for 2 s and 1 s, respectively. N_2 was pulsed for 30 s during the deposition in order to separate H_2O from TMA completely. The growth rate of Al_2O_3 film was approximately 1 Å per cycle.

After deposition, the samples were annealed by using an RTA oven at temperatures ranging from 700 °C to 1000 °C for 1 min. The heating rates were all set up at 30 °C/s and the cooling rate can reach 25 °C per second through the cooling equipment. The RTA processing was carried out in a 99.999%-purity N_2 atmosphere. The morphologies of the as-deposited and the post-annealed Al_2O_3 films were obtained by using atomic force microscopy (AFM) in a tapping mode. The thickness values of a variety of post-annealed Al_2O_3 films were determined by variable angle spectroscopic ellipsometry (VASE) made in the J. A. Woollam Co., Inc. instrument covering the spectral range from 192 nm to 1500 nm. Other papers [13,14] presented just a few measured data of thickness and refractive index of annealed samples. We determined the crystallization temperature point more accurately and narrowed the window of the crystallization process, so more annealing temperatures were carried out and measured. We first annealed the sample from 700 °C to 1000 °C in steps of 50 °C. The 750-°C annealing was imposed on as-deposited Al_2O_3 sample, and we found that its thickness was a little thinner than that of the as-deposited sample, which implied that the crystallization just began. When the annealing temperature was 800 °C, the thickness almost reached a minimal limiting value. So we selected middle values between 750 °C and 800 °C to elaborate the experiment. We selected 768 °C and 785 °C as the additional annealing temperatures. The micro-structures of as-deposited and annealed Al_2O_3 films were characterized by synchrotron radiation light source using grazing incidence x-ray diffraction (GIXRD) with a wavelength of 1.238 Å. XPS was performed under ultrahigh vacuum condition (base pressure in the analysis chamber was 1×10^{-9} mbar, 1 bar = 10^5 Pa) by an ESCALAB 250 electron spectrometer equipped with monochromated Al Kα radiation ($h\nu = 1486.8$ eV) and a hemispherical electron analyzer. The Ar sputtering was used to etch Al_2O_3 film layer-by-layer and the incident angle of Ar was 40° with respect to the normal of Al_2O_3 surface. After each etching step, photoelectrons of O 1s, Ar 2p, and Al 2p were collected in sequence and the exit angle was the normal to the surface. The scanning step of high resolution spectrum was 0.05 eV and the passing energy was 30 eV. During collection, charge calibration was used to eliminate charge accumulation caused by the continuous Ar sputtering. All the XPS spectra were calibrated by Ar 2p, whose peaks are located at 241.9 eV and 244.02 eV.[15]

3. Results and discussion

3.1. Thickness and refractive index

The thickness values and refractive indexes of as-deposited and annealed ALD Al_2O_3 films on SiC epitaxial wafers are measured by VASE using Cauchy model as shown in Fig. 1. We can obviously see that the thickness and refractive index of 650 °C are similar to those of pre-annealed Al_2O_3 sample. The thickness of the as-grown Al_2O_3 film is measured to be 487 Å, which does not decrease greatly until its annealing temperature reaches 750 °C. When the annealing temperature increases to 768 °C, the thickness reduces to 442 Å, which is 90.7% of the as-deposited Al_2O_3 film. From 750 °C to 768 °C, the thickness decreases sharply and becomes smooth at 800 °C, which is 88.9% of the as-deposited Al_2O_3 film thickness. Although temperature increases successively, the thickness does not reduce largely any more. Thickness reduction often occurs for ALD Al_2O_3 films, which is due to densification of the film.[3] To sum up, from the annealing temperature 750 °C to 768 °C, the sample has completed the process of structural transition from amorphous phase to polycrystalline phase. The largest thickness change generally occurs at temperatures of the crystallization point, i.e., 768 °C in this work.[16]

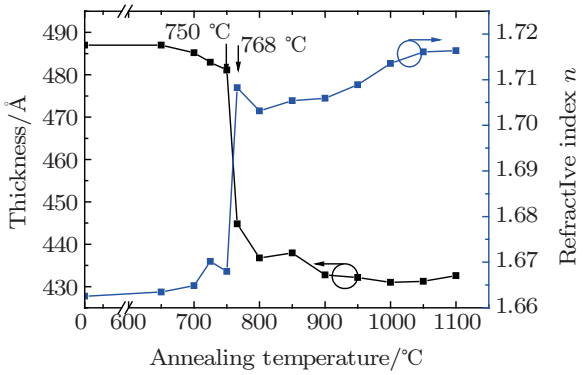


Fig. 1. (color online) Variations of thickness and refractive index (at a wavelength of 632 nm) of Al_2O_3 film with annealing temperature for 1 min in N_2 atmosphere.

In the annealing process, the denser the film, the larger the refractive index is.[17] When the annealing temperature is lower than 750 °C, the refractive index at a wavelength of 632 nm is 1.665. Subsequently, the refractive index increases to approximately 1.705, when the annealing temperature increases from 768 °C to 950 °C. The refractive index reaches to 1.715 for further increasing temperature from 950 °C to 1100 °C. According to Gladstone–Dale equation,[18] the relationship between refractive index and density is expressed

as

$$\rho = K(n-1), \tag{1}$$

where ρ is the density and K is a constant which means that the film density is directly proportional to refractive index n. The increase of refractive index is due to the enhancement of the densification upon annealing. The previous report[19] demonstrated that the Al_2O_3 film is amorphous with low reflective index (1.66–1.67), while the high one (1.71) indicates that the film is crystalline. These results demonstrate that the film completes the structural transition from amorphous phase to crystalline phase upon the RTA.

3.2. Morphology analysis

The surface morphologies of as-deposited and annealed Al_2O_3 films characterized by AFM are shown in Figs. 2(a)–2(d). It can be seen that surface of as-deposited Al_2O_3 film is very smooth with few grains as shown in Fig. 2(a). When the annealing process is performed at 750 °C as shown in Fig. 2(b), the surface becomes rough and there are grains (15 nm in diameter) formed on the film surface, which indicates that the annealed Al_2O_3 films start to crystallize. The grains are growing (23 nm at 768 °C and 30 nm at 1000 °C) and gradually become uniformly distributed with the increase of the annealing temperature as shown in Figs. 2(c) and 2(d), which demonstrates that the crystallization of the Al_2O_3 film is completed. Figure 3 presents root-mean-square (RMS) roughness of Al_2O_3 film as a function of annealing temperature. The RMS roughness of as-deposited Al_2O_3 film is 0.34 nm, which is similar to that of annealed Al_2O_3 film at 768 °C. Then the RMS value presents a linear increase from 0.43 nm to 0.54 nm under the annealing condition from 800 °C to 1000 °C. It can be confirmed that the surface reconstruction in the annealing process is responsible for the roughening of annealed Al_2O_3 film.[20] The surface feature accompanied by crystallization is confirmed by GIXRD as follows.

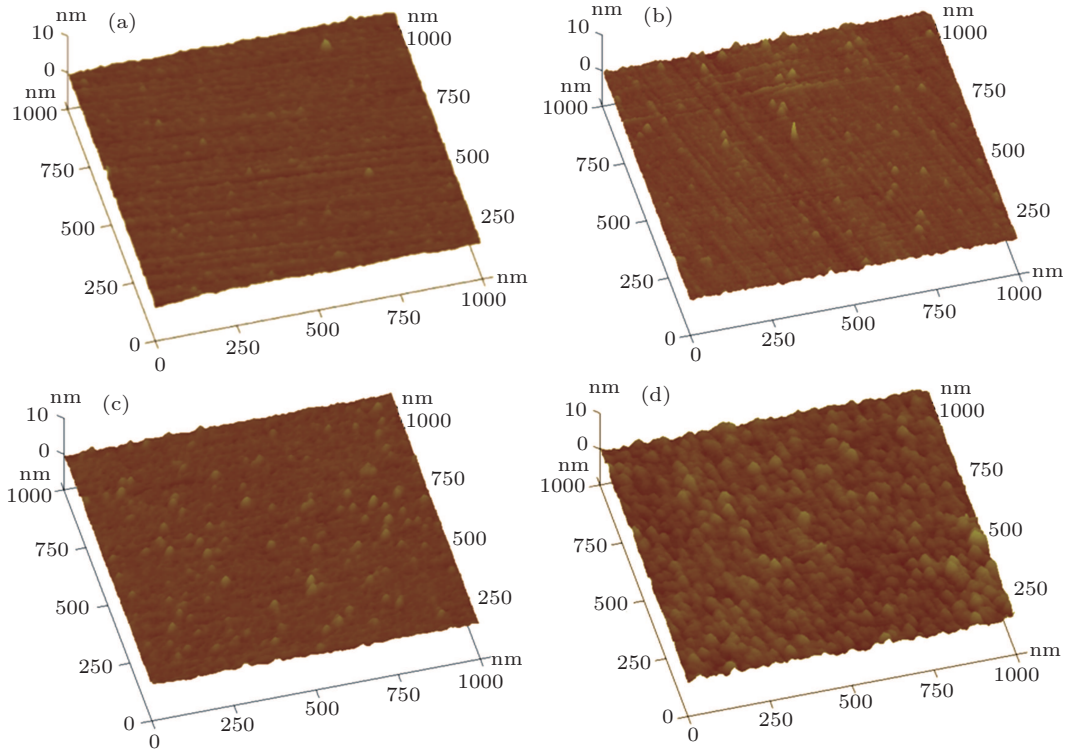


Fig. 2. (color online) Three-dimensional AFM images (1 μm× 1 μm) of (a) as-deposited Al_2O_3 film and after annealing at (b) 750 °C, (c) 768 °C, and (d) 1000 °C for 1 min in N_2 atmosphere.

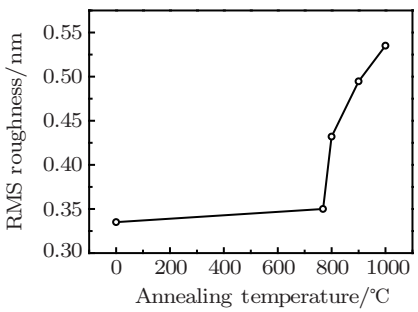


Fig. 3. Root-mean-square (RMS) roughness of Al_2O_3 films with different annealing temperatures.

3.3. Micro-structure analysis

Figure 4 shows the variations of GIXRD patterns with annealing temperature of Al_2O_3 films. The spectrum of as-deposited Al_2O_3 film shows an amorphous phase similar to that of the annealed film at 750 °C as shown in Fig. 4. No diffraction peak is observed, which indicates that the film does not start to crystallize. When the Al_2O_3 film is annealed at a temperature of 850 °C, some diffraction peaks can be observed, including reflection planes of (111), (511), and (440),

which are corresponding to 15.75°, 47.65°, and 52.5°, respectively. According to JCPDS (joint committee on powder diffraction standards) Card, the crystalline structure of the annealed Al_2O_3 film belongs to γ-Al_2O_3. The intensity of peak at 52.8 has no difference from those at higher temperature (950 °C and 1050 °C), indicating that the crystallization has already been completed at 850 °C.[21,22] The intensities of peaks at 47.65 and 15.75 from higher temperature (950 °C and 1050°) annealing samples indeed are a little stronger than those at lower temperatures (750 °C and 850 °C). This is most likely to be due to preferential orientation along the (111) and (511) planes.[23,24] This suggests that during higher temperature annealing, the (111) and (511) planes are better crystallized. The GIXRD results confirm that the Al_2O_3 film transits from amorphous phase to crystalline phase when being annealed at above 750 °C. The films under XRD measurements each have a thickness of 50 nm. Under such a thin film, the photoelectron signal from Al_2O_3 film will be smaller than that from a normal bulk material. Therefore, the crystallinity seen from GIXRD spectrum is weak. On the other hand, the strong crystallization film consists of many grain boundaries, which may be a route to increasing the leakage current when applied by a voltage.[25]

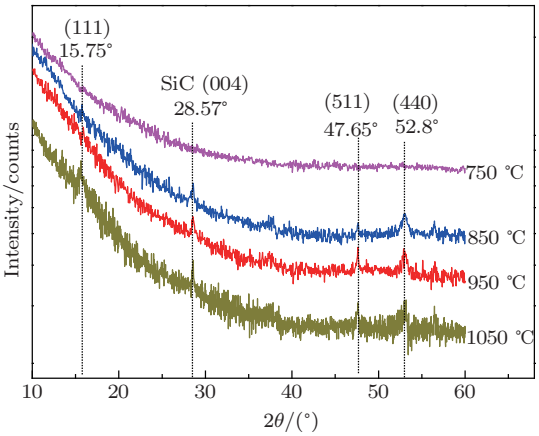


Fig. 4. (color online) GIXRD patterns of Al_2O_3 films annealed at temperatures ranging from 750 °C to 1050 °C for 1 min in N_2 atmosphere.

3.4. Composition analysis

XPS spectra are carried out on both as-deposited and annealed samples. XPS sputter-depth profiling is carried out to determine the element distribution in both samples each as function of depth near the Al_2O_3/SiC interface. The thickness values of as-deposited and annealed Al_2O_3 film are 31.6 nm and 27.4 nm, respectively. For the two samples, the interface of annealed Al_2O_3 film needs more time to be detected than that of the as-deposited film. The sputter rates of as-deposited sample and annealed sample are, respectively, about 0.256 Å/S and 0.17 Å/S, which indicates that the Al_2O_3 film becomes much denser after being annealed.

The detailed Al 2p spectra of as-deposited and annealed samples are compared in Fig. 5. Gaussian function is used to fit the measured curves. As shown in Figs. 5(a)–5(f), the first four Al 2p spectra away from the interface can be fitted by one peak perfectly. The peaks of the fitted curves are all 74.79 eV, which corresponds to Al–O bonding.[26,27] When the thickness approaches to the interface thickness (31 nm, (e)), the intensity of the Al 2p decreases greatly and the full width of half maximum (FWHM) of fitted curves becomes larger than those of previous fitted curves, which indicates that the film quality deteriorates and some nonstoichiometric features and impurity appear. When the thickness comes to 33 nm, the peak of Al 2p must be fitted by two Gaussian peaks, which are located at 74.79 eV and 73.8 eV, respectively. Kim *et al.*[28] reported that the Al_2O_3 grown by ALD using H_2O as resource has a binding energy of 72.8 eV considered to be for Al–Al bonding. According to ALD growing mechanism the component centered at 73.8 eV is assigned to Al–O–Si bonding. Meanwhile, as shown in Figs. 5(g)–5(l) from the annealed sample, the first two spectra (Figs. 5(g)–5(h)) are fitted by one peak located at 74.95 eV for Al 2p of the annealed sample, which is a little larger than 74.79 eV of as-deposited Al–O bonding. After being annealed, the film transits from amorphous phase to crystalline phase, thus Al 2p shifts to a higher binding energy.[4] The Al 2p spectra from Figs. 5(i)–5(k) are fitted by one peak, which is smaller than the above two and almost the same as the peak of the as-deposited sample. This phenomenon suggests that annealing does not influence the Al 2p near the interface or the interface is still amorphous when being annealed. The Al 2p in Fig. 5(l) has two peaks: one is 74.79 eV corresponding to Al–O, and the other is 73.8 eV corresponding to Al–O–Si compound. There is not much difference in chemical bonding between as-deposited and annealed sample at the interface.

Figure 6 shows O 1s spectra corresponding to Al 2p spectra of various sputtering thickness from as-deposited and annealed samples. The first four spectra (Figs. 6(a)–6(d)) can be fitted by one peak located at 531.36 eV perfectly, which indicates that only Al–O bonding exists in the film. The O 1s curves in Figs. 6(e) and 6(f) are fitted by three Gaussian curves. One of the three fitted peaks corresponds to Al–O bonding, and the two others are located at 531.88 eV and 533.1 eV, respectively. According to some papers[14,29] Al–OH bonding which is often found in Al_2O_3 film grown by ALD has a 1.3 eV–1.4 eV shift to higher binding energy relative to Al–O bonding. It is obvious that no peak is centered around 532.7 eV, corresponding to Al-OH bonding. At the interface, Al–O–Si bonding is inevitable during growing as a transition layer between Al_2O_3 film and SiC substrate.[14] The electronegativity of Si is larger than that of Al, such a peak at 531.88 eV is assigned to Al–O–Si bonding relative to Al–O–Al bonding centered at 531.36 eV. In addition, Al–O–Si bonding just exists near the interface, therefore the Al–O–Si component is controlled by growing mechanism not the growing parameter.

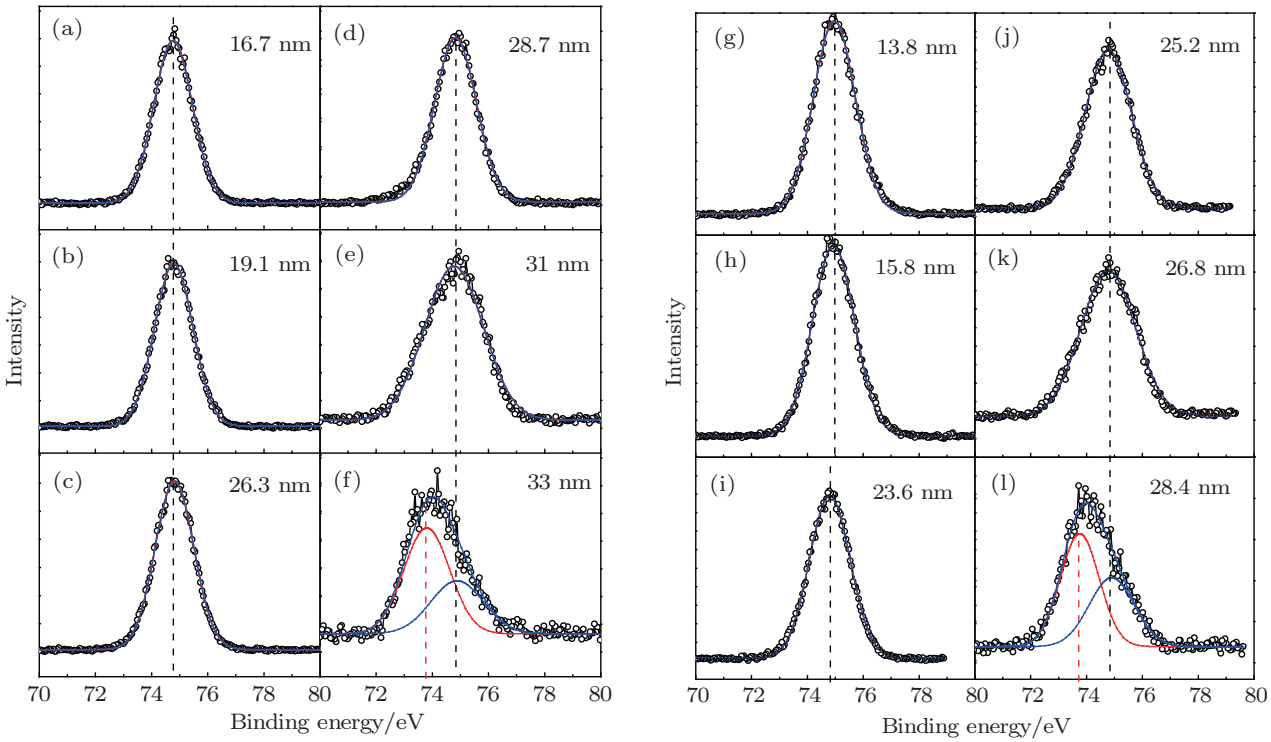


Fig. 5. (color online) Narrow Al 2p XPS profiles of different etching thickness from the as-deposited ((a)–(f)) and 1000 °C annealed ((g)–(l)) Al_2O_3 samples.

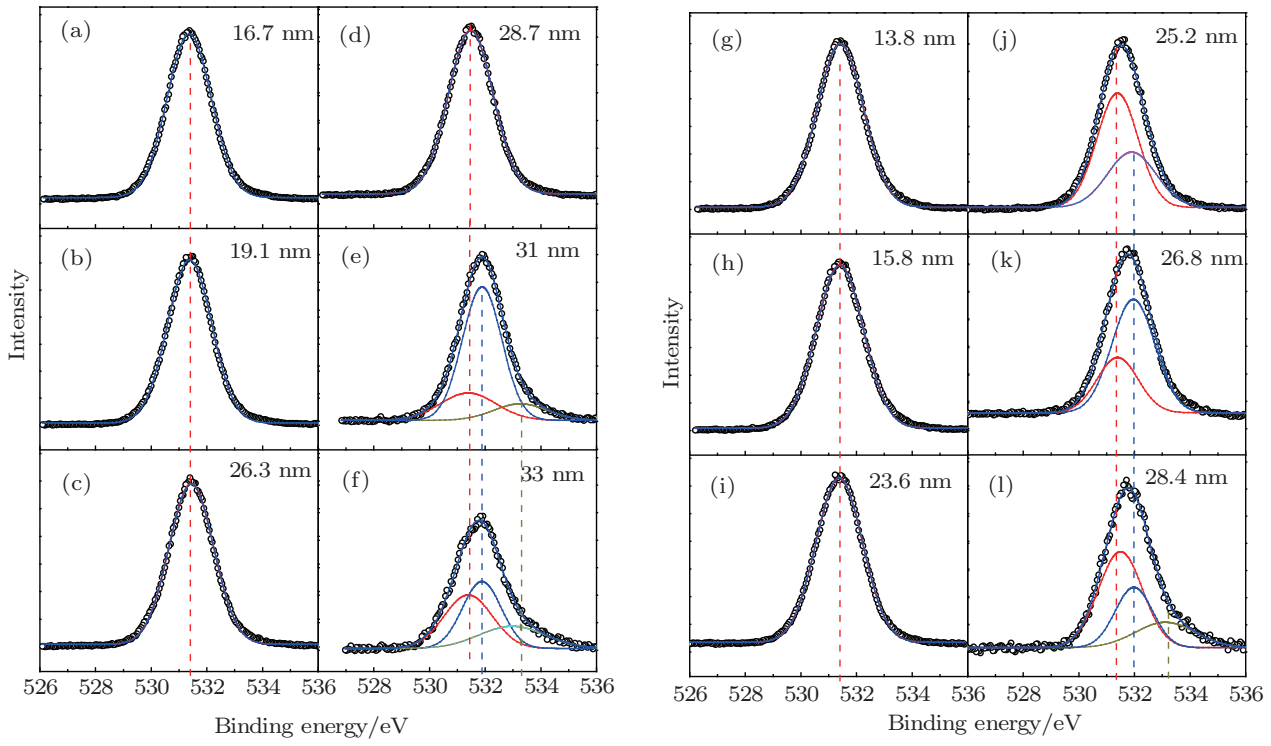


Fig. 6. (color online) Narrow O 1s XPS profiles of different etching thickness from the as-deposited ((a)–(f)) and 1000 °C annealed ((g)–(l)) Al_2O_3 samples.

Figures 6(g)–6(l) show the XPS profiles of O 1s in the annealed samples. The O 1s in Figs. 6(g)–6(i) can be fitted by one peak located at 531.44 eV, which is a little larger than the peak of as-deposited film. The symmetry of O 1s spectra suggests that O atoms fully join in Al–O–Al bonds. The O 1s spectra from Figs. 6(j) and 6(k) are fitted by two spectra. One is Al-O bond at 531.44 eV and the higher binding energy at 531.88 eV is assigned to Al–O–Si bonding, which only exists at the interface and is similar to that of the as-deposited sample. The curve from Fig. 6(l) is fitted by three spectra and the peak at 533.1 eV that does not appear in Fig. 6(k) belongs to C–O bonding. After the sample is annealed, less C–O bonds remain at the surface and most of the C–O bonds escape from the surface.

The peak of Al 2p spectrum shifts from 74.79 eV to 74.95 eV after the sample has been annealed, while the binding energy of O 1s changes from 531.36 eV to 531.44 eV. It should be noticed that the energy separations between Al 2p and O 1s ($\Delta E_{\mathrm{Al,O}}$) of as-deposited and annealed film are 456.57 eV and 456.49 eV, respectively. These two energy separations are both close to 456.6 eV reported for sapphire in Ref. [29]. A similar energy separation means a similar Al–O bonding state,[10,29] indicating that the short range ordering of amorphous film and that of crystalline film are close to each other. The binding energy shifts of Al 2p and O 1s after the sample has been annealed are both attributed to the film transition from amorphous phase to crystalline γ-Al_2O_3, which is associated with long range ordering of Al_2O_3 film. The first-neighbor Al–O bonding is related to short range ordering and the second-nearest-neighbour coordination O–O bonding (or Al–Al bonding) dominates long range ordering.

Combined with thickness analyses of various temperatures, film densification (equivalent to the reduction of free volume) occurs accompanied with film crystallization. The binding energy shifts of Al 2p and O 1s and unaltered $\Delta E_{\mathrm{Al,O}}$ indicate that first-neighbour Al–O bond distance is not the reason for densification, but the translocation of O–O (or Al–Al) second-nearest-neighbour coordination is responsible for film densification.[29] However, the reduced binding energy of Al 2p in Fig. 5(i) indicates that long range ordering near interface is unchanged during annealing. The interface still keeps short range ordering but not long range ordering. These results are also consistent with the statements that the interface is amorphous.

4. Conclusions

In this work, Al_2O_3 films are prepared by using atomic layer deposition based on SiC epitaxial wafer and followed by fast temperature annealing. The Al_2O_3 films each have a fine morphology with low RMS even after being annealed. With annealing temperature increasing, the film thickness decreases continuously but for annealing temperatures between 750 °C–768 °C, the thickness has a sharp reduction, meanwhile crystallization happens. The binding energies of Al 2p and O 1s increase together after crystallization by almost the same value. The long range ordering (second-nearest-neighbor coordination variation) is responsible for atom binding energy shift. The nearest-neighbor coordinations are similar between as-deposited and annealed Al_2O_3, resulting from the same separation of Al 2p and O 1s. At the interface, the similar Al 2p binding energy and chemical bonds upon annealing suggest that annealing does not have much influence and the interface is still amorphous.

Acknowledgment

The GIXRD experiments were conducted on the Shanghai Synchrotron Radiation Facility (SSRF) BL14B1 for determining the phase of Al_2O_3 films, for which we are grateful to the SSRF team.

References

[1] Baliga B J 2005 *Silicon Carbide Power Devices* (Singapore: World Scientific)
[2] Avice M, Diplas S, Thogersen A, Christensen J S, Grossner U, Svensson B G, Nilsen O, Fjellvag H and Watts J F 2007 *Appl. Phys. Lett.* **91** 052907
[3] Tanner C M, Toney M F, Lu J, Blom H O, Sawkar-Mathur M, Tafesse M A and Chang J P 2007 *J. Appl. Phys.* **102** 104112
[4] Zhang F, Sun G, Zheng L, Liu S, Liu B, Dong L, Wang L, Zhao W, Liu X, Yan G, Tian L and Zeng Y 2013 *J. Appl. Phys.* **113** 044112
[5] Afanasev V V, Bassler M, Pensl G and Schulz M 1997 *Phys. Status Solidi A* **162** 321–337
[6] Lipkin L A and Palmour J W 1999 *IEEE Trans. Electron Dev.* **46** 525
[7] Zhang X H, Domercq B, Wang X D, Yoo S, Kondo T, Wang Z L and Kippelen B 2007 *Org. Electron.* **8** 718
[8] Puurunen R L 2005 *J. Appl. Phys.* **97** 121301
[9] Ritala M, Leskelä M, Dekker J P, Mutsaers C, Soininen P J and Skarp J 1999 *Chem. Vap. Deposition* **5** 7
[10] Diplas S, Avice M, Thogersen A, Christensen J S, Grossner U, Svensson B G, Nilsen O, Fjelivag H, Hinderc S and Watts J F 2008 *Surf. Interface Anal.* **40** 822
[11] Grossner U, Servidori M, Avice M, Nilsen O, Fjellvag H, Nipoti R and Svensson B G 2007 *Silicon Carbide and Related Materials* 2006 **556–557** 683
[12] Tanner C M, Sawkar-Mathur M, Lu J, Blom H O, Toney M F and Chang J P 2007 *Appl. Phys. Lett.* **90** 061916
[13] Jakschik S, Schroeder U, Hecht T, Gutsche M, Seidl H and Bartha J W 2003 *Thin Solid Films* **425** 216
[14] Avice M, Grossner U, Pintilie I, Svensson B G, Servidori M, Nipoti R, Nilsen O and Fjellvag H 2007 *J. Appl. Phys.* **102** 054513
[15] F M J, J C and C k R 1995 *Handbook of X-ray Photoelectron Spectroscopy: a reference book of standard spectra for identification and interpretation of XPS data* (Minnesota: Physical Electronics, Inc.)
[16] Cimalla V, Baeumler M, Kirste L, Prescher M, Christian B, Passow T, Benkhelifa F, Bernhardt F, Eichapfel G, Himmerlich M, Krischok S and Pezoldt J 2014 *Mater. Sci. Appl.* **5** 628
[17] Shih K K 1994 *J. Vac. Sci. Technol. A* **12** 321
[18] Gladstone J H and Dale T P 1863 *Philos. Trans. R. Soc. London* **153** 317
[19] Ott A W, Klaus J W, Johnson J M and George S M 1997 *Thin Solid Films* **292** 135
[20] Qin H, Sutter P, Zhou G and Jacobson N 2014 *J. Am. Ceram. Soc.* **97** 2762
[21] Zhang L, Jiang H C, Liu C, Dong J W and Chow P 2007 *J. Phys. D: Appl. Phys.* **40** 3707
[22] Zhao C, Roebben G, Bender H, Young E, Haukka S, Houssa M, Naili M, De Gendt S, Heyns M and Van Der Biest O 2001 *Microelectron. Reliab.* **41** 995
[23] Banakh O, Schmid P E, Sanjines R and Levy E 2003 *Surf. Coat. Tech.* **163** 57
[24] Ishihara M, Li S J, Yumoto H, Akashi K and Ide Y 1998 *Thin Solid Films* **316** 152
[25] Tanner C M, Perng Y C, Frewin C, Saddow S E and Chang J P 2007 *Appl. Phys. Lett.* **91** 203510
[26] Yang W S, Kim Y K, Yang S Y, Choi J H, Park H S, Lee S I and Yoo J B 2000 *Surf. Coat. Tech.* **131** 79
[27] Jung Y C, Miura H, Ohtani K and Ishida M 1999 *J. Cryst. Growth* **196** 88
[28] Kim J B, Kwon D R, Chakrabarti K, Lee C, Oh K Y and Lee J H 2002 *J. Appl. Phys.* **92** 6739
[29] Snijders P C, Jeurgens L P H and Sloof W G 2005 *Surf. Sci.* **589** 98